Thin Solid Films 690 (2019) 137517

Contents lists available at ScienceDirect

Thin Solid Films

journal homepage: www.elsevier.com/locate/tsf

Influence of film thickness on the dielectric characteristics of hafnium oxide layers

D.A. Golosov[a,*], N. Vilya[a], S.M. Zavadski[a], S.N. Melnikov[a], A.V. Avramchuk[b], M.M. Grekhov[b], N.I. Kargin[b], I.V. Komissarov[a]

[a] Belarusian State University of Informatics and Radioelectronics, 6 P. Brovka str., 220013 Minsk, Belarus
[b] National Research Nuclear University MEPhI, 31 Kashmirskoye Ave., Moscow 115409, Russia

ARTICLE INFO

Keywords:
Amorphous thin film
High-k dielectric
Hafnium oxide
Reactive magnetron sputtering
Dielectric characteristics

ABSTRACT

The present work focuses on the study of properties of hafnium oxide (HfO_2) films, deposited by reactive magnetron sputtering of the Hf target in Ar/O_2 gas mixture. The X-ray diffraction analysis of the deposited films proved the amorphous structure of the films, which was also confirmed by the Raman spectroscopy.

It was determined that as the HfO_2 film thickness had been decreased from 98.6 nm to 13.5 nm, film density had dropped from 9.52 to 9.26 g/cm^2. At the same time, the dielectric constant dropped from 21.3 to 8.0 units, and the dielectric loss tangent rose, especially at high frequencies. At the same time, the decrease in film thickness resulted in increased leakage currents at low electric field density *E*, and decreased leakage currents at high *E*. Improvement of dielectric characteristics and increase in leakage current with film thickness growth is a consequence of film densification and the formation of a crystalline phase. Thickness dependence of the dielectric constant is associated with the violation of the ionic polarization mechanism at the film electrode interface.

1. Introduction

The main goal of the development of up-to-date microelectronics is to reduce the topological size of semiconductor elements in order to achieve the maximum packing density, maximum operational speed and minimum power consumption of integrated circuits. Increasing the degree of the integrated circuits integration density is mainly achieved through the use of the scaling principle – a proportional reduction of the geometric dimensions of the elements. According to this principle, a decrease in the length of a metal-oxide-silicon field-effect transistor (MOSFET) channel is accompanied by a decrease in the thickness of the gate dielectric. First of all, this occurs due to the need to suppress short-channel effects in a MOSFET. The trend is explained as follows. When reducing the channel length in order to prevent channel depletion, it is necessary to increase the doping level of the substrate. An increase in the doping concentration of the substrate leads to an increase in the threshold voltage of the transistor and a decrease in carrier mobility, which reduces the drain current. Reducing the threshold voltage is achieved by increasing the gate capacitance by thinning the gate dielectric.

Silicon oxide has been used as the key dielectric in silicon integrated circuits over the course of the microelectronics evolution. However, further application of SiO_2 has some principal limitations associated with low dielectric constant of this material ($\varepsilon \approx 3.9$). In the first MOSFET, the thickness of SiO_2 was about 100 nm. With each new generation of IC, the length of the transistor channel had been decreasing and, accordingly, so had been the thickness of the gate dielectric. As a result, the technology-specific standards of 60 nm demand the MOSFET gate dielectric thickness to be reduced down to 1.2 nm being approximately 5 atomic layers thick [1]. With the further reduction of dielectric film thickness, its insulation properties degrade considerably due to the dramatic growth of tunnel leakage currents. High leakage currents lead to unacceptably large additional power dissipation and a decrease in the slope of the current-voltage characteristic of the transistor. Therefore, the transition to the scaled down technology-specific standards demands the use of novel materials, characterized by high dielectric constant – so-called alternative or *high-k* dielectrics [2]. The formation of a gate dielectric from a material with a high dielectric constant allows for the increase in its thickness, while maintaining the gate capacitance at the same level. Simultaneously, leakage currents are reduced by several orders of magnitude compared to a thinner SiO_2 dielectric.

* Corresponding author at: Electronic Technique and Technology Department, Center 10.1, Thin Film Research Laboratory, P. Brovka str. 6, 220013 Minsk, Belarus.
E-mail address: dmgolosov@gmail.com (D.A. Golosov).

https://doi.org/10.1016/j.tsf.2019.137517
Received 31 October 2018; Received in revised form 6 August 2019; Accepted 20 August 2019
Available online 21 August 2019
0040-6090/ © 2019 Published by Elsevier B.V.

Presently, the following metal oxides are investigated as *high-k* dielectrics to be used in MOSFET devices: hafnium oxide HfO_2 ($\varepsilon \approx 25$), zirconium oxide ZrO_2 ($\varepsilon \approx 25$), titanium oxide TiO_2 ($\varepsilon \approx 80$), aluminum oxide Al_2O_3 ($\varepsilon \approx 10$), and tantalum oxide Ta_2O_5 ($\varepsilon \approx 22$) [3–5]. However, the value of the dielectric constant is not the only important characteristic for the application of new materials in microelectronics. Important characteristics are also the band gap energy, band offsets with silicon for both electrons and holes, leakage currents, and the breakdown field strength. From this point of view, hafnium oxide has attracted much more attention from recent researches, since it combines a high dielectric constant [1] and a large band gap of E_g = 5.6–5.8 eV, which is higher than that of other *high-k* materials [3,6]. The band offsets of HfO_2 with silicon for both electron and hole is 1.5 and 3.4 eV, respectively. This band alignment is acceptable and also better than other high-k dielectrics [3]. In addition, hafnium oxide has a high thermal stability and thermodynamic compatibility at the interface with silicon (the free energy of reaction with Si is about 199.3 kJ/mol) [3,8,9].

However, as of today, the practical application of *high-k* dielectric films in microelectronics faces serious problems due to the lack of compatible technologies for reproducible deposition of thin *high-k* dielectric films. Nowadays, a number of technologies are used to grow HfO_2 films, such as thermal oxidation [10,11], atomic layer deposition [12,13], chemical vapor deposition [14], pulsed laser deposition [15,16], DC and RF sputtering [17–20], and sol-gel methods [21–24]. Thus, the films are applied onto heated substrates or subjected to subsequent annealing, most often because of peculiarities of the above processes. However, hafnium oxide exhibits insufficient thermal stability and tends to crystallize at temperatures of 400–450 °C [25,26]. The crystallization brings about a number of defects to the structure of polycrystalline films, which causes the increase of leakage current at the grain boundaries [26,27]. Recent research has proved that dielectrics with low crystallization have improved dielectric properties when compared to those with strong crystallization phase [28]. One of the methods to form amorphous dielectrics is based on the processes that allow the film to be deposited under low temperatures and with a minimal power effect on the growing film. The reactive magnetron sputtering is a low-temperature process, that enables the deposition of high-quality thin oxide films from metallic target with controllable stoichiometric properties over large areas. The method has also a number of other advantages compared to the methods listed above, including high purity and low-cost manufacturing. However, the issue is the ability to grow ultra-thin (up to 20 nm) amorphous hafnia films with good dielectric characteristics using this technique.

Therefore, the objective of this paper is to study the properties of amorphous HfO_2 films, obtained by reactive magnetron sputtering without heating the substrate, to establish the relation between the film thickness and the dielectric properties of the film and to find the possibility of using these films as gate dielectrics in MOSFET devices.

2. Experiment

The diagram of the experimental setup used for the deposition of hafnium oxide thin films by reactive magnetron sputtering is provided in Fig. 1. The chamber of the vacuum setup was equipped with the magnetron sputtering system MAC-80 with the ∅ 80-mm target and the clearing ion source based on a Hall current accelerator.

The HfO_2 films were deposited to the substrates of high-alloy monocrystalline silicon Si (111). During the experiments, the substrates were placed on a rotary substrate holder 85 cm away from the magnetron target surface. The chamber of the vacuum setup was pumped down to the residual pressure of 10^{-3} Pa, and the ion precleaning of substrates was performed in order to remove the surface impurities and a natural oxide film from the surface of the silicon substrates. For this purpose, the working gas Ar was fed to the ion source up to the working pressure of 0.02 Pa. The cleaning time, ion energy and discharge current were constant during all of the experiments: 6 min (substrate holder rotary mode), 500 eV, and 70 mA, respectively.

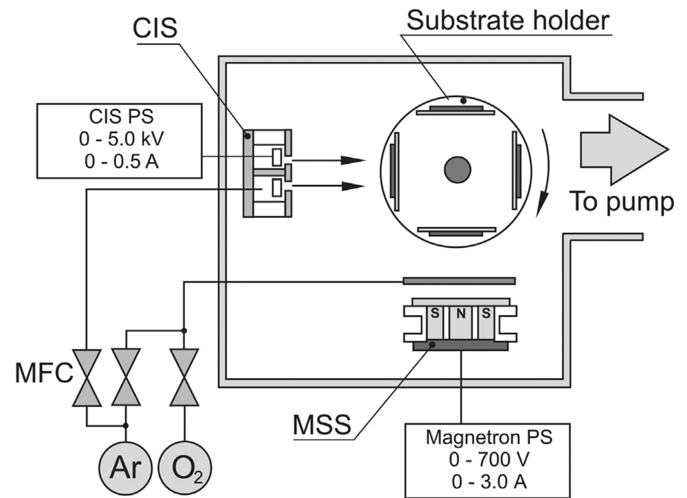

Fig. 1. Diagram of the experimental setup for HfO_2 film deposition by reactive magnetron sputtering technique (MSS – magnetron sputtering system, CIS – clearing ion source, MFC – mass flow controller, PS – power supply).

Then, the HfO_2 films were deposited. For this purpose, the substrates were placed in the deposition area one by one. Hf target (99.6% purity) of 2 mm in thickness was sputtered in Ar/O_2 mixture. The working gases were supplied to the gas-distribution system of the magnetron. The flows of Ar and O_2 for all the experiments were preserved constant at Q_{Ar} = 50 sccm, Q_{O2} = 10 sccm. The mass flow controllers RRG-1 maintained the gas flow rate at a given level. During the sputtering process, the discharge current of the magnetron was kept constant at I_t value of 1.4 A, and the discharge voltage was 480 V. In these modes the deposition rate was about 1.2 nm/s. The thickness of the films deposited was controlled through changing the deposition time and varied from 13.5 to 98.6 nm.

The structure of the films was determined by means of X-ray diffraction (XRD) with X-ray diffractometer *Ultima IV* (*Rigaku*) in CuK_α-radiation. The X-ray patterns were obtained at the room temperature within the angular range of 2θ = 20–120°. The X-ray reflectometry (XRR) method was applied to evaluate the surface roughness of the deposited film, its thickness and density. The measurements were carried out when the incident parallel beam was formed with special-purpose optics and a double-reflection monochromator crystal (Ge (220) × 2). In addition, the following beam-forming slits were used: 10-mm vertical slit at the primary beam, then 0.1 mm horizontal slit; and two 0.2-mm slits and a Soller slit (0.5) for the diffracted beam (0.5) in order to reduce divergence. The scanning range was 0.1° – 7° with a step of 0.004°. Simulation and more precise determination of HfO_2 layer parameters were carried out using GlobalFit processing package.

The Raman scattering spectra were obtained using *Confotec NR500* scanning confocal microscope with a laser excitation of 2.62 eV (473 nm) in the back-scatter geometry and under normal environmental conditions with spectral resolution of 3 cm^{-1}. Scanning electron microscopy (SEM) images were obtained using a Hitachi S-4800 high resolution field emission scanning electron microscope at accelerating voltage 15.0 kV. The method of ellipsometry was employed to analyze the thickness of the deposited films (ellipsometer LEF-3 M-1) with the incidence beam angle being 65° to the normal.

The dielectric characteristics of the film were verified on the test metal-oxide-semiconductor structures. For this purpose, the top Ni electrode was deposited on the HfO_2 film through a mask. The area of capacitors was 0.096 mm^2. The capacitance, the dielectric loss tangent and the volt-ampere characteristic were obtained using the LCR meter E7–20 at 25–10^6 Hz. The dielectric constant values were calculated

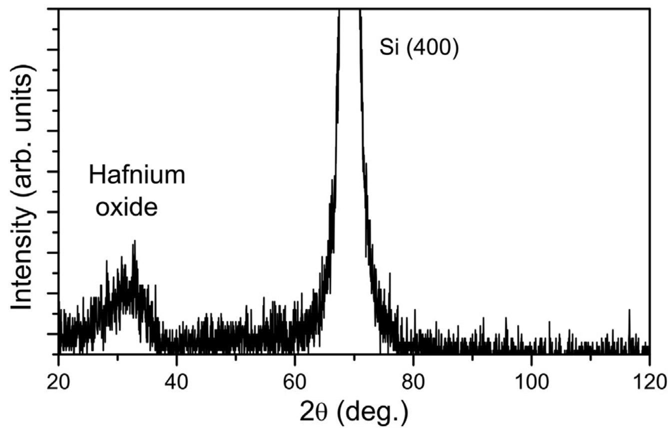

Fig. 2. Diffraction pattern of the HfO_2/Si structure (sample HfO_2–4).

using the dielectric thickness and the total capacitance of the capacitor structure using the below expression

$$\varepsilon = \frac{Cd}{\varepsilon_0 S} \quad (1)$$

where C – is the capacitance of the capacitor, d – thickness of the hafnium oxide film, S – area of the capacitors, ε_0 – electric constant $\varepsilon_0 = 8.85 \times 10^{-12}$ F/m.

3. Results and discussion

XRD method was used to study the structure of the deposited films. The analysis of the XRD patterns proved that the as-deposited HfO_2 film were amorphous (Fig. 2). Diffraction patterns contained the reflex of monocrystalline Si (400). Within the region of angles $2\theta = 28°– 31°$, where the reflexes corresponding to different phases of crystalline HfO_2 were supposed to be present, there was a wide diffusion hump of low intensity (full width at half maximum was 7°). That hump is usually accounted for by the amorphous structure [29], which, by definition, is associated with a substance without a long-range order, but with possible local close-range order at a distance from one to two bond lengths. In order to confirm the amorphous state of the HfO_2, the deposited films were also subject to the Raman spectroscopy (Fig. 3). The spectra obtained were compared to the Raman spectra of the initial Si substrate. The absence of additional peaks on the Raman spectrum also proved the amorphous structure of the HfO_2 films.

XRR method was used to evaluate the density of the deposited material, its thickness and the surface roughness. The approximation

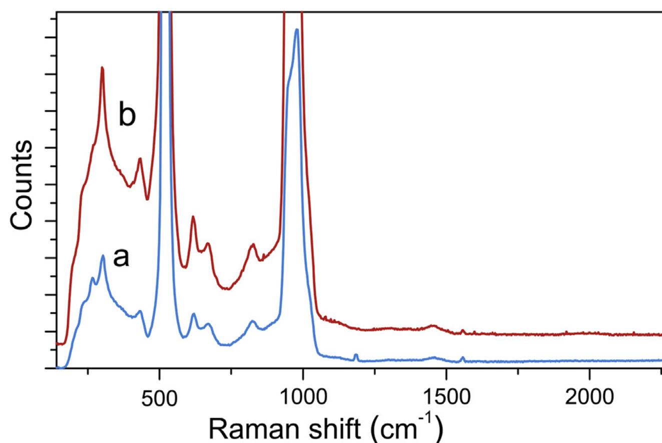

Fig. 3. Raman scattering spectrum of the initial Si substrate (a) and HfO_2/Si structure (b) (sample HfO_2–4).

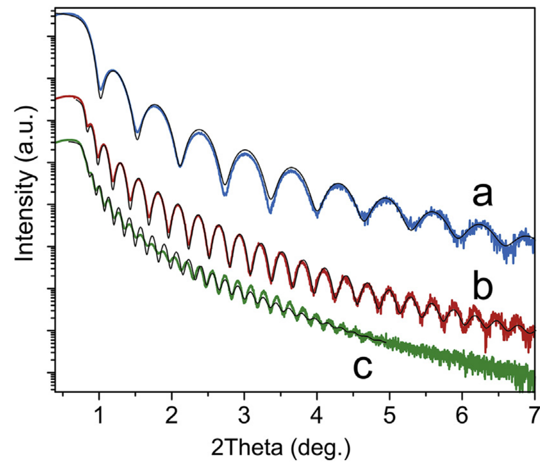

Fig. 4. Experimental (color) and fitted (black) XRR curves for various HfO_2 film thicknesses: a – 13.5 nm, b – 29.6 nm, c – 98.6 nm.

results for the experimental curves obtained through film reflectometry of HfO_2 films are presented in Fig. 4. During simulation the adjustment parameter χ^2 for all the samples did not exceed 0.01 (see Table 1). The received parameters of the HfO_2 films obtained are reviewed in Table 1. In addition, the method of ellipsometry was applied to specify the thickness of the deposited films. The values of the film thickness received were in good correlation with the XRR data (ref. Table 1). The density of the deposited films was within the range of 9.26–9.52 g/cm^2 and had been growing as the film thickness increased. A lower film density, if compared to the density of the bulk material (ρ_{HfO2} = 9.68 g/cm^3), was probably also the consequence of the amorphous structure of the deposited samples. The film surface roughness did not exceed 0.3 nm, being comparable with the roughness of the initial substrate. The study of the film morphology by atomic force microscopy confirmed low surface roughness of the samples (Fig. 5). Thus, the XRR, SEM and ellipsometry data analysis proved that the films deposited were characterized by low surface roughness, high continuity and the absence of islands, being true even for 13.5 nm samples.

The analysis of the dielectric constant and dielectric loss tangent vs. frequency curves demonstrated that dielectric constant was higher at lower frequencies for all of the samples, if compared to that at higher frequencies (Fig. 6). While the HfO_2 film was 98.6 nm in thickness, the dielectric constant ε at 1 kHz was over 21.3 units. As the film thickness was going down, ε was also decreasing, and reached 8.0 units with the film thickness of 13.5 nm. When the film reached the thickness of 98.6 nm, the dielectric loss tangent $tg\varphi$ remained within the 0.02–0.03 margin (Fig. 7) for all the frequency range. As the film thickness dropped, the value of $tg\varphi$ was observed to grow, especially at high frequencies. As the film thickness hit 13.5 nm, $tg\varphi$ reached 0.27 at 1 MHz.

Fig. 8 plots the leakage current density vs. electric field intensity $J_L(E)$ curves for HfO_2 films. With zero bias, the leakage current density for all the samples was about 10^{-7}A/cm^2. As for 13.5 nm samples, while the E grew, the leakage currents dramatically increased up to 10^{-4} A/cm^2 and then gradually grew up to 10^{-3} A/cm^2 at $E = 1.5 \times 10^6$ V/cm. As the film was getting thicker, the leakage currents were observed to drop down at lower values of the filed strength. However, at large values of the electric field strength ($E = 1.5 \times 10^6$ V/cm) the leakage currents increased up to 10^{-1} A/cm^2. The dielectric breakdown also depended on the HfO_2 film thickness. For 13.5 nm films, the breakdown field strength was about 4.5×10^6 V/cm. As the film thickness increased, the breakdown field strength dropped down to $(1.8–2.0) \times 10^6$ V/cm with the film being 98.6 nm thick.

The evaluation of the findings confirms that the dielectric properties of the HfO_2 films deposited by reactive magnetron sputtering are

Table 1
XRR and ellipsometry results of HfO_2 films.

Sample №	Deposition time, sec	Thickness, nm		Roughness, nm	Density, g/cm^3
		XRR (χ^2)	Ellipsometry		
HfO_2-1	10	13.5 (0.009)	13.7	0.236	9.26
HfO_2-2	25	29.6 (0.009)	29.2	0.297	9.34
HfO_2-3	30	39.6 (0.082)	36.4	0.232	9.39
HfO_2-4	40	48.8 (0.079)	46.8	0.287	9.44
HfO2-5	85	101.6 (0.004)	98.6	0.235	9.52

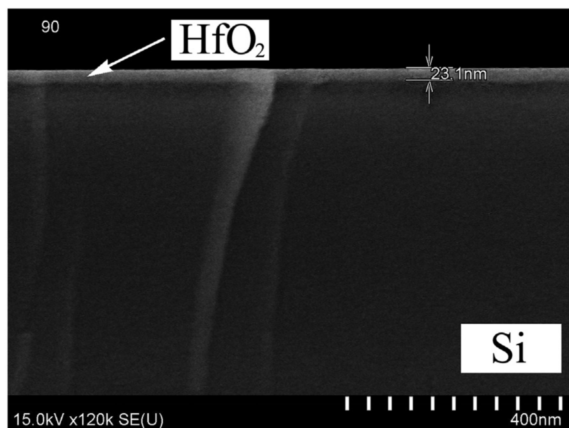

a

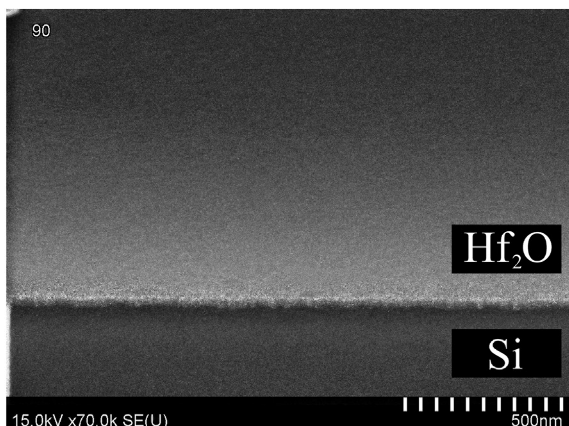

b

Fig. 5. SEM images of cross-section (*a*) and surface (*b*) of the HfO_2 film on Si substrate (sample HfO_2–2).

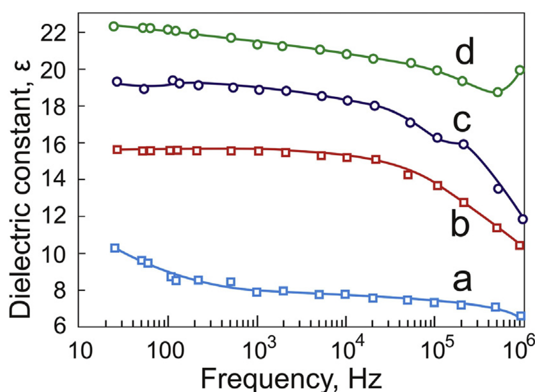

Fig. 6. Dielectric permittivity vs. frequency curves for different HfO_2 film thicknesses: *a* – 13.5 nm, *b* – 29.6 nm, *c* – 48.8 nm, *d* – 98.6 nm.

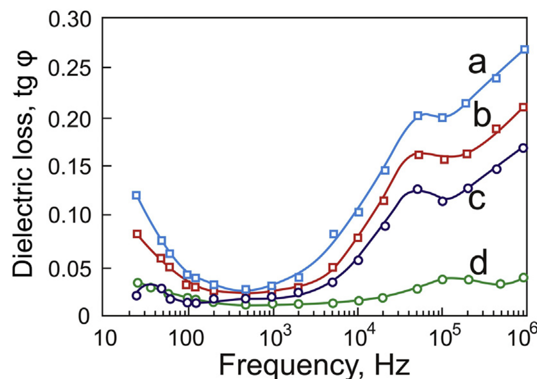

Fig. 7. Dielectric loss tangent vs frequency curves for various HfO_2 film thicknesses: *a* – 13.5 nm, *b* – 29.6 nm, *c* – 48.8 nm, *d* – 98.6 nm.

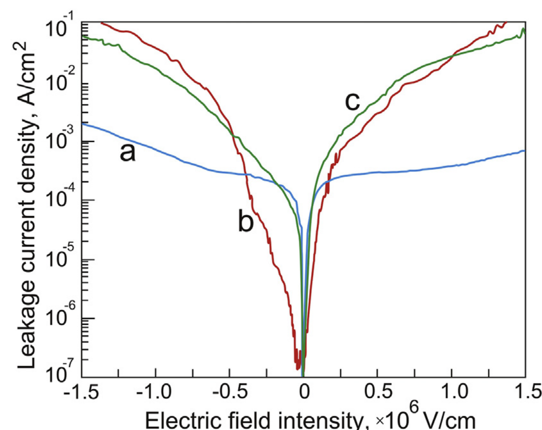

Fig. 8. Leakage current density vs. electric field intensity curves for various thicknesses of HfO_2 films: *a* – 13.5 nm, *b* – 29.6 nm, *c* – 98.6 nm.

determined by the film thickness. As the film thickness decreases, ε is observed to go down, and $tg\varphi$ grows, especially at high frequencies. Additionally, as the film thickness decreases, the leakage current density rises with low electric field strength, and J decreases with high E. Thus, for the films with a thickness of 13.5 nm, an almost three times decrease in ε compared to films with a thickness of 98.6 nm was observed. Some authors attributed the decrease in permittivity to the formation of a boundary layer (hafnium monoxide, SiO_2 or hafnium silicate) at the film-substrate interface, which has lower value of ε and decreases the effective dielectric constant value [30]. However, the analysis in [31] of ultra-thin HfO_2 films deposited by the method of magnetron sputtering without heating the substrate showed that there was no boundary layer at the interface with silicon. Also, no boundary layers were found in ultra-thin Gd_2O_3 films deposited by electron beam evaporation without heating the substrates [32]. The formation of a boundary layer was detected only when films were deposited on heated substrates or after annealing [33,34]. It was also suggested that the effective dielectric constant of the film decreases due to a reduction in

the density of the films and an increase in the volume of voids [35]. However, in our case, the XRR and SEM results showed that even with a small film thickness, they have low surface roughness and high surface continuity. The decrease in the density of the films with a decrease in their thickness did not exceed 3%. Therefore, we assume that the decrease in the dielectric constant of the films is not related to the properties of the material and is a consequence of the size effects [36]. The dielectric constant of the films is typically determined by the permanent, ionic and electronic polarizations. Full polarization is the sum of these values. In high-k materials, the dominant polarization mechanism is ionic polarization. However, in a capacitor, at the boundaries with contacts, the mechanism of ionic polarization may be disturbed, which is associated with a change in the structure of the film [36]. This leads to a decrease in the effective dielectric constant, and this effect is especially pronounced in ultra-thin films [37].

These changes of leakage current density are associated with differences in the growth mechanisms of thin and thicker films. While film thickness remains low, the hafnia is unable to crystallize and remains amorphous. The film structure is characterized by a close-range order only, and there are no grain boundaries in the film [38]. As the film thickness increases, there appears to be a possibility that nuclei of crystallization will form. Further increase in the film thickness will boost further formation of new crystallization nuclei and growth of the present crystal. As a result of crystallization, the film density becomes greater. Variations in $J(E)$ characteristics are associated with the differences in the current transfer mechanisms in amorphous and partially crystallized films. In thin films, the leakages are most probably determined by direct tunneling of the carriers. As the film thickness increases, the flow of charge along the grain boundaries becomes the main current transfer mechanism [39].

4. Conclusion

Amorphous HfO_2 films were deposited by reactive magnetron sputtering of the Hf target in Ar/O_2 mixture of gases. It has been established that the deposited films are characterized by low surface roughness and high surface continuity, even when the film is ultrathin. A thorough study of the dielectric properties of the HfO_2 films deposited by this technique demonstrated that without the heating of the substrates and its further annealing, the films were characterized by the dielectric constant such as $\varepsilon = 21.3$, and dielectric loss tangent of 0.018 at 1.0 kHz, with leakage current being 10^{-2} A/cm at $E = 10^6$ V/cm. When the film thickness decreases, ε is reduced, and $tg\varphi$ increases, especially at high frequencies. While the film was 13.5 nm thick, ε was 8.0 units, and $tg\varphi = 0.032$. In addition, in thinner films, the leakage current density grows with low electric field intensity, and J drops down at high E. The decrease of dielectric loss in thicker films are most likely the consequence of the increasing film density and formation of the crystalline phase in thicker films. Thickness dependence of the dielectric constant is associated with a violation of the mechanism of ionic polarization at the film electrode interface.

A combination of amorphous microstructure and excellent dielectric properties allow these films to be used as *high-k* dielectrics in integrated metal-oxide-silicon capacitors and field effect transistors. It is worth mentioning that the reactive magnetron sputtering process is a low-temperature process. This, together with high deposition rates of HfO_2 films, makes it possible to employ the reactive magnetron sputtering technique for film deposition onto polymer substrates.

Acknowledgements

The authors are grateful to P.L. Dobrokhotov (National Research Nuclear University MEPhI) for the assistance with XRR experiments and discussions.

References

[1] J. Robertson, R.M. Wallace, High-K materials and metal gates for CMOS applications, Mater. Sci. Eng. R. Rep. 88 (2014) 1–41, https://doi.org/10.1016/j.mser.2014.11.001.
[2] S. Hall, O. Buiu, I.Z. Mitrovic, Y. Lu, W.M. Davey, Review and perspective of high-k dielectrics on silicon, J. Telecomun. Inform. Technol. 2 (2007) 33–43.
[3] J. Robertson, B. Falabretti, Band offsets of high K gate oxides on III-V semiconductors, J. Appl. Phys. 100 (2006) 014111–1 – 014111-8, https://doi.org/10.1063/1.2213170.
[4] G. Ribes, J. Mitard, M. Denais, S. Bruyere, F. Monsieur, C. Parthasarathy, E. Vincent, G. Ghibaudo, Review on high-k dielectrics reliability issues, IEEE Trans. Device Mater. Reliab. 5 (1) (2005) 5–19, https://doi.org/10.1109/TDMR.2005.845236.
[5] J. Robertson, High dielectric constant oxides, Eur. Phys. J. Appl. Phys. 28 (2004) 265–291, https://doi.org/10.1051/epjap:2004206.
[6] V.V. Afanas'ev, A. Stesmans, F. Chen, X. Shi, S.A. Campbell, Internal photoemission of electrons and holes from (100) Si into HfO_2, Appl. Phys. Lett. 81 (2002) 1053–1055, https://doi.org/10.1063/1.121930.
[8] C.M. Lopez, N.A. Suvorova, E.A. Irene, A.A. Suvorova, M. Saunders, ZrO2 film interfaces with Si and SiO2, J. Appl. Phys. 98 (3) (2005) 033506–1 – 6, https://doi.org/10.1063/1.1994938.
[9] H.H. Zhang, C.Y. Ma, Q.Y. Zhang, Scaling behavior and structure transition of ZrO2 films deposited by RF magnetron sputtering, Vacuum 83 (11) (2009) 1311–1316, https://doi.org/10.1016/j.vacuum.2009.04.041.
[10] M. Wu, Y.I. Alivov, H. Morkoc, High-k dielectrics and advanced channel concepts for Si MOSFET, J. Mater. Sci. Mater. Electron. 19 (2008) 915–951, https://doi.org/10.1007/s10854-008-9713-2.
[11] Y. Xie, Z. Ma, Y. Su, Y. Liu, L. Liu, H. Zhao, J. Zhou, Z. Zhang, J. Li, E. Xie, The influence of mixed phases on optical properties of HfO_2 thin films prepared by thermal oxidation, J. Mater. Res. 26 (1) (2011) 50–54, https://doi.org/10.1557/jmr.2010.61.
[12] J. Gao, G. He, J.W. Zhang, Y.M. Liu, Z.Q. Sun, Deposition temperature dependent optical and electrical properties of ALD HfO_2 gate dielectrics pretreated with tetrakisethylmethylamino hafnium, Mater. Res. Bull. 70 (2015) 840–846, https://doi.org/10.1016/j.materresbull.2015.06.016.
[13] J. Gao, G. He, Z. Sun, H. Chen, C. Zheng, P. Jin, D. Xiao, M. Liu, Modification of electrical properties and carrier transportation mechanism of ALD derived HfO_2/Si gate stacks by Al_2O_3 incorporation, J. Alloys Compd. 667 (2016) 352–358, https://doi.org/10.1016/j.jallcom.2016.01.171.
[14] A. Devi, S. Cwik, K. Xu, A.P. Milanov, H. Noei, Y. Wang, D. Barreca, J. Meijer, D. Rogalla, D. Kahn, R. Cross, H. Parala, S. Paul, Rare-earth substituted HfO_2 thin films grown by metalorganic chemical vapor deposition, Thin Solid Films 520 (2016) 4512–4517, https://doi.org/10.1016/j.tsf.2011.10.141.
[15] A.G. Bagmut, I.A. Bagmut, V.A. Zhuchkov, M.O. Shevchenko, Phase transformations in films deposited by laser ablation of Hf in an oxygen atmosphere, Tech. Phys. 57 (2012) 856–860, https://doi.org/10.1134/S1063784212060035.
[16] H. Liu, G. Wang, Z. Zhang, K. Pan, X. Zeng, Synthesis of negative thermal expansion HfW_2O_8 thin film using pulsed laser deposition, Ceram. Int. 40 (9) (2014) 13855–13859, https://doi.org/10.1016/j.ceramint.2014.05.103.
[17] L. Qi, R. Han, L. Liu, H. Sun, Preparation and magnetic properties of DC-sputtered porous HfO_2 films, Ceram. Int. 42 (16) (2016) 18925–18930, https://doi.org/10.1016/j.ceramint.2016.09.042.
[18] K.C. Das, N. Tripathy, S.P. Ghosh, P. Sharma, R. Singhal, J.P. Kar, Microstructural, surface and interface properties of zirconium doped HfO_2 thin films grown by RF co-sputtering technique, Vacuum. 143 (2017) 288–293, https://doi.org/10.1016/j.vacuum.2017.06.022.
[19] S.S. Lin, C.S. Liao, Structure and physical properties of W-doped HfO_2 thin films deposited by simultaneous RF and DC magnetron sputtering, Surf. Coat. Technol. 232 (2013) 46–52, https://doi.org/10.1016/j.surfcoat.2013.04.051.
[20] N. Manikanthababu, M. Dhanunjaya, S.V.S. Rao, A.P. Pathak, SHI induced effects on the electrical and optical properties of HfO_2 thin films deposited by RF sputtering, Nucl. Inst. Methods Phys. Res. B 379 (2016) 230–234, https://doi.org/10.1016/j.nimb.2016.01.042.
[21] P. Jin, G. He, D. Xiao, J. Gao, M. Liu, J. Lv, Y. Liu, M. Zhang, P. Wang, Z. Sun, Microstructure, optical, electrical properties, and leakage current transport mechanism of sol-gel processed high-kHfO_2 gate dielectrics, Ceram. Int. 42 (6) (2016) 6761–6769, https://doi.org/10.1016/j.ceramint.2016.01.050.
[22] T.P. Smirnova, L.V. Yakovkina, V.O. Borisov, Impact of lanthanum on the modification of HfO_2 films structure, J. Rare Earths 33 (8) (2015) 857–862, https://doi.org/10.1016/S1002-0721(14)60496-8.
[23] K. Tetzner, K.A. Schroderb, K. Bock, Photonic curing of sol–gel derived HfO_2 dielectrics for organic field-effect transistors, Ceram. Int. 40 ((2014) 15753–15761, https://doi.org/10.1016/j.ceramint.2014.07.099.
[24] X. Yan, D. Su, H. Duan, F. Zhang, Preparation of SiOC/HfO_2 fibers from silicon alkoxides and tetrachloride hafnium by a sol–gel process, Mater. Lett. 148 (2015) 196–199.
[25] V. Mikhelashvili, R. Brener, O. Kreinin, J. Shneider, G. Eisenstein, Characteristics of metal-insulator-semiconductor capacitors based on high-k HfAlO dielectric films obtained by low-temperature electron-beam gun evaporation, Appl. Phys. Lett. 85 (2004) 5950–5952, https://doi.org/10.1063/1.1836875.
[26] F.M. Li, B.C. Bayer, S. Hofmann, J.D. Dutson, S.J. Wakeham, M.J. Thwaites, W.I. Milne, A.J. Flewitt, High-k (k = 30) amorphous hafnium oxide films from high rate room temperature deposition, Appl. Phys. Lett. 98 (2011) 252903–1 – 252903-3, https://doi.org/10.1063/1.3601487.
[27] J.H. Choi, Y. Mao, J.P. Chang, Development of hafnium based high-k materials – a

review, Mater. Sci. Eng. R. Rep. 72 (6) (2011) 97–136, https://doi.org/10.1016/j.mser.2010.12.001.

[28] W.J. Choi, E.J. Lee, K.S. Yoon, J.Y. Yang, J.H. Lee, C.O. Kim, J.P. Hong, Annealing effects of HfO_2 gate thin films formed by inductively coupled sputtering technique at room temperature, J. Korean Phys. Soc. 45 (2004) S716–S719.

[29] M. Modreanu, J. Sancho-Parramon, D. O'Connell, J. Justice, O. Durand, B. Servet, Solid phase crystallisation of HfO_2 thin films, Mater. Sci. Eng. B 118 (2005) 127–131, https://doi.org/10.1016/j.mseb.2004.12.068.

[30] U. Saxena, O.N. Srivastava, Unusual thickness dependence of the dielectric constant of erbium oxide films, Thin Solid Films 33 (2) (1976) 185–192, https://doi.org/10.1016/0040-6090(76)90079-1.

[31] B.H. Lee, L. Kang, R. Nieh, W.-J. Qi, J.C. Lee, Thermal stability and electrical characteristics of ultrathin hafnium oxide gate dielectric reoxidized with rapid thermal annealing, Appl. Phys. Lett. 76 (2000) 1926–1928, https://doi.org/10.1063/1.126214.

[32] J. Kwo, M. Hong, A.R. Kortan, K.L. Queeney, Y.J. Chabal Jr., R.L. Opila, D.A. Muller, S.N.G. Chu, B.J. Sapjeta, T.S. Lay, J.P. Mannaerts, T. Boone, H.W. Krautter, J.J. Krajewski, A.M. Sergnt, J.M. Rosamilia, Properties of high k gate dielectrics Gd_2O_3 and Y_2O_3 for Si, J. Appl. Phys. 89 (2001) 3920–3927, https://doi.org/10.1063/1.1352688.

[33] Bing-Yue Tsui, Hsiu-Wei Chang, Formation of interfacial layer during reactive sputtering of hafnium oxide, J. Appl. Phys. 93 (12) (2003) 10119–10124, https://doi.org/10.1063/1.1574594.

[34] A. Callegari, E. Cartier, M. Gribelyuk, H.F. Okorn-Schmidt, T. Zabel, Physical and electrical characterization of Hafnium oxide and Hafnium silicate sputtered films, J. Appl. Phys. 90 (2001) 6466–6674, https://doi.org/10.1063/1.1417991.

[35] D. Deger, K. Ulutas, Conduction and dielectric polarization in Se thin films, Vacuum 72 (2004) 307–312, https://doi.org/10.1016/j.vacuum.2003.08.008.

[36] K. Natori, D. Otani, N. Sano, Thickness dependence of the effective dielectric constant in a thin film capacitor, Appl. Phys. Lett. 73 (5) (1998) 632–634, https://doi.org/10.1063/1.121930.

[37] D. Deger, K. Ulutas, Comparison of dielectric dispersion of Al_2O_3 and Se thin films, J. Appl. Physiol. 89 (2001) 8101–8104, https://doi.org/10.1063/1.1372161.

[38] D.C. Gilmer, R. Hegde, R. Cotton, R. Garcia, V. Dhandapani, Compatibility of polycrystalline silicon gate deposition with HfO_2 and Al_2O_3/HfO_2 gate dielectrics, Appl. Phys. Lett. 81 (2002) 1288–1290, https://doi.org/10.1063/1.1499514.

[39] A.A. Rastorguev, V.I. Belyi, T.P. Smirnova, L.V. Yakovkina, M.V. Zamoryanskaya, V.A. Gritsenko, H. Wong, Luminescence of intrinsic and extrinsic defects in hafnium oxide films, Phys. Rev. B 76 (2007), https://doi.org/10.1103/PhysRevB.76.235315 235315-1 – 235315-6.